https://scilett-fsg.uitm.edu.my/
Science Letters, **14**(2): 71-84 (2020)

ISSN: 1675-7785
eISSN: 2682-8626
DOI: 10.24191/sl.v14i2.9544

Silver(I) Dicyanonitrosomethanide, $Ag[ONC(CN)_2]$ Complex as Catalyst for the Selective Oxidation of Styrene to Benzaldehyde

Mohammad Anwar Mohamed Iqbal[1], Muhammad Zulhelmi Nazri[1], Mohammad Norazmi Ahmad[2], Erna Normaya Abdullah[2], Umie Fatihah Mohamad Haziz[1], Mohd Rizal Razali[1], Farook Adam[3]

[1]School of Chemical Sciences, Universiti Sains Malaysia, 11800 Penang, Malaysia

[2]Experimental and Theoretical Research Lab, Department of Chemistry, Kulliyyah of Science, International Islamic University Malaysia, Bandar Indera Mahkota, 25200 Kuantan Pahang, Malaysia

Corresponding author: anwariqbal@usm.my

Received: 13 February 2020; Accepted: 29 March 2020; Published: 1 June 2020

ABSTRACT

Silver(I) dicyanonitrosomethanide, $Ag[ONC(CN)_2]$ represent a 3D interwoven coordination polymer organization in which all the donor atoms of the functional groups of $ONC(CN)_2^-$ are coordinated to the Ag(I). Oxidation of styrene utilizing H_2O_2 as an oxidant in acetonitrile (CH_3CN) was used as a model reaction to investigate the catalytic potential of the Ag(I) complex. The CH_3CN was chosen as the solvent based on the data collected from Conductor like Screening Model for Real Solvents (COSMO-RS) study. The data indicate that the Ag[ONC(CN)2] complex was compatible and soluble in CH_3CN. Different parameters such as styrene:H_2O_2 molar ratio, reaction time, catalyst mass, and reaction temperature were studied. Highest styrene conversion (36%) with 100% selectivity towards benzaldehyde (BZ) was achieved when 25 mg catalyst, 1:1 styrene to H_2O_2 molar ratio were used. The reaction was carried out at 303 K for 3 h. The catalytic conversion of styrene to BZ is proposed to take place *via* [Ag-H_2O_2] adduct with styrene oxide (StO) as an intermediate. Molecular Electrostatic Potential (MEP) shows that the Ag atom has the highest probability to coordinate with the oxygen atom of H_2O_2. The MEP data confirms the proposed mechanism.

Keywords: *Styrene oxidation; Silver(I) dicyanonitrosomethanide; COSMO-RS; Molecular electrostatic potential (MEP)*

https://scilett-fsg.uitm.edu.my/
Science Letters, **14**(2): 71-84 (2020)

ISSN: 1675-7785
eISSN: 2682-8626
DOI: 10.24191/sl.v14i2.9544

INTRODUCTION

Chemical industries have been using benzaldehyde as an intermediate in perfumery, dyestuff, pharmaceuticals, resin additives and in organic synthesis [1-3]. Oxidation of benzyl alcohol, direct oxidation of toluene, hydrogenation of benzoic acid, indirect electro-oxidation of toluene and hydrolysis of benzyl chloride are among the processes that have been used to synthesize benzaldehyde [4-7]. These methods require complicated synthesis processes, expensive raw materials and may cause severe environmental pollution. Besides that, the catalytic conversion was low, and the selectivity towards benzaldehyde was poor as well. Compared to heterogeneous catalysts, homogeneous catalysts can give higher catalytic activity under milder conditions. In homogeneous catalysis, all the catalytic sites are easily accessible due to the solubility of the metal complex. Also, the chemoselectivity, regioselectivity, and enantioselectivity of the metal complex can easily be tuned [8]. High conversion of styrene with good selectivity toward benzaldehyde had been achieved using metal complexes containing vanadium (V) [9], Cu(II) [10], Ln(III) [11] and many more.

The nitrosodicyanomethanide, $ONC(CN)_2^-$ which is an analog of the $C(CN)_3^-$ anion has received considerable attention due to its ability to act as multidentate bridges in various 3D metal complexes [12]. Bohle and co-workers [13] reported that the dicyanonitrosomethanide anion is a better π-acceptor as an *N*-bound ligand and a better σ-donor as an *O*-bound ligand. Besides, Hvastijová and co-workers [14] found that the $[ONC(CN)_2]^-$ anion can act as a bidentate bridging ligand by utilizing its cyano nitrogen for the binding mode. The dicyanonitrosomethanide salts have significantly smaller C–C bond distance and a longer $C–N_{nitroso}$ bond distance, indicating unique features present in the anion [15].

The structure of Silver(I) dicyanonitrosomethanide, $Ag[ONC(CN)_2]$ was first reported in the 1970s by Chow et al. [16], but the precise ligand bond length could not be determined accurately. Glover et al. [12] were able to determine the geometry of the ligand more accurately. The anion was reported to be tetracoordinated with the Ag(I) metal center *via* three nitrogen atoms (two of the CN groups and one of the nitroso group) and the oxygen atom of the nitroso group in a distorted tetrahedral form. The crystal structure and bond lengths of the complex was discussed in detail by Glover et al. [12]. Various types of Ag single crystals have been identified to have strong interaction with styrene and styrene oxide. However, to the best of our knowledge, the catalytic potential of $Ag[ONC(CN)_2]$ in the oxidation of styrene has not been reported.

Thus, in this study, the catalytic potential of $Ag[ONC(CN)_2]$ complex was investigated in the selective styrene oxidation to benzaldehyde with H_2O_2 as an oxidant. The studied parameters were styrene:H_2O_2 molar ratio, reaction time, catalyst mass and reaction temperature. A reaction mechanism was proposed based on the data collected. Conductor like Screening Model for Real Solvents (COSMO-RS) and Molecular Electrostatic Potential (MEP) were done to analyze the compatibility of the $Ag[ONC(CN)_2]$ complex in the acetonitrile (CH_3CN) and to identify the highest potential electrophile region during the oxidation process, respectively.

https://scilett-fsg.uitm.edu.my/
Science Letters, **14**(2): 71-84 (2020)

ISSN: 1675-7785
eISSN: 2682-8626
DOI: 10.24191/sl.v14i2.9544

EXPERIMENTAL

Materials

Styrene (Sty) ($C_6H_5CH=CH_2$, Merck, 99%), 30% hydrogen peroxide (H_2O_2, Qrëc), acetonitrile (CH_3CN, Lab Scan, 99.5%), sodium nitrite ($NaNO_2$, Merck), malononitrile ($CH_2(CN)_2$, Merck), glacial acetic acid (CH_3COOH, ChemAR), methanol (CH_3OH, Qrëc), silver nitrate ($AgNO_3$, Sigma-Aldrich) and ascorbic acid ($C_6H_8O_6$, Biochemical) were analytical grade and obtained from commercial sources and used as received without further purification.

Synthesis of Silver(I) Dicyanonitrosomethanide, Ag[ONC(CN)$_2$] complex

The procedures reported by Glover et al. [12] was used for the synthesis of Silver(I) dicyanonitrosomethanide, Ag[ONC(CN)$_2$] complex. A solution of $NaNO_2$ (1.0 g, 14.49 mmol) and 10 mL of distilled water was slowly added to a stirring solution of $CH_2(CN)_2$ (0.5 g, 7.57 mmol) and 5 mL of glacial CH_3COOH. The mixture was refluxed for 3 h at room temperature before adding the $AgNO_3$ (1.3 g, 7.67 mmol). The precipitate formed was isolated by filtration, washed with distilled water and CH_3OH and dried under vacuum to give Ag[ONC(CN)$_2$] complex.

Liquid phase oxidation of styrene

The oxidation of styrene was carried out according to the method described by Adam and Iqbal with some modifications [17]. In a typical experiment, 10 mmol of Sty, 10 mL of CH_3CN and catalyst (25 mg, 50 mg, 75 mg or 100 mg) were mixed in a 50 mL round bottom flask and heated to the 303 K. The H_2O_2 (10 mmol) was added to the flask, and the reaction was continued for 3 h. Aliquots (0.5 mL) of the reaction mixture was withdrawn every hour and subjected to GC and GC-MS analyses.

Instrumentations

The FTIR-ATR spectrum of the complex was recorded in the range 600-4000 cm^{-1} using Perkin Elmer FT-IR Microscope Spotlight 200 (USA). The UV-Vis spectrum of the sample dissolved in CH_3CN was recorded using Perkin Elmer Lambda 35 UV-Vis spectrophotometer (USA) over a range of 350 – 700 nm at room temperature. The CHN elemental analysis was carried out on a Perkin Elmer Series II, 2400 microanalyzer (USA). The melting point of the complex was determined using a GallenKamp instrument (India). Gas chromatograph (GC) analysis of the products was done using PerkinElmer Clarus 500 (USA) equipped with a capillary wax column (30 m length and 0.25 mm inner diameter) and FID detector. Products were identified using Perkin Elmer Clarus 600 (USA) gas chromatography–mass spectrometry (GC–MS) equipped with the same column.
Computational Approach

The behavior of the complex in CH_3CN and the effect of the functional groups on electronic properties was investigated through σ-profile using COSMO-RS. Optimization of the Ag[ONC(CN)$_2$] and the CH_3CN was the first step toward predicting the thermodynamic properties using COSMO-RS. The geometries and the continuum solvation COSMO calculations of the solvent molecular surface density and the complex were optimized using DFT calculations with Becke-Perdew-86 (BP86) functional and triple zeta valance potential (TZVP) basis sets. Then, the COSMO-files containing the ideal screening charges on the

https://scilett-fsg.uitm.edu.my/
Science Letters, **14**(2): 71-84 (2020)

ISSN: 1675-7785
eISSN: 2682-8626
DOI: 10.24191/sl.v14i2.9544

molecular surface were generated and used to create the sigma profile and the polarity of the complex. All the quantum calculation above was carried out using Amsterdam Density Functional (ADF) program package, version 2017 [18]. The Gaussian 09 suite was used to optimize the geometrical parameters of $Ag[ONC(CN)_2]$ by using the DFT B3LYP 6-31 ++ G (d,p) in polarized continuum model (PCM). This basis set was chosen due to their efficiencies in calculating the polar bonds of $Ag[ONC(CN)_2]$. The optimized structure was chosen from the stable conformation and been applied to the Molecular Electrostatic Potential (MEP) study [18, 19].

RESULTS AND DISCUSSION

Synthesis and characterization of $Ag[ONC(CN)_2]$ complex

The calculated and experimentally obtained elemental data of $Ag[ONC(CN)_2]$ complex are given in Table 1. The calculated and experimental values are almost similar, indicating that the synthesized complex is pure.

Table 1: The physical characteristics and elemental analysis of $Ag[ONC(CN)_2]$ complex. The calculated values are given in parenthesis.

Complex	Physical Appearance	Yield (%)	Melting Point (°C)	Elemental analysis (%)		
				C	H	N
$Ag[ONC(CN)_2]$	Yellow	92.3	210 (decomposes)	17.8 (17.6)	0.0 (0.0)	20.7 (20.5)

The FTIR spectrum of the $Ag[ONC(CN)_2]$ complex is shown in Figure 1. Only the main peaks of the complex are discussed. The stretching band for imine functional group (C=N) can be observed at 1683 cm^{-1} [19]. The two bands at 2246 cm^{-1} and 2229 cm^{-1} are attributed to the stretching vibration of the cyano group ν(C≡N). These two peaks seem to be overlapping and not well resolved. The IR bands around 1334 cm^{-1} correspond to the in-plane stretching vibration of ν(C-N), ν(N-O) and the asymmetric stretching vibration of the CNO bond. The in-plane stretching vibrations of ν(C=N) and the bending vibrations of the nitroso group δ(C-N-O) and also ν(CNO) are shown by the presence of the bands at 1292 cm^{-1}. The band at 814 cm^{-1} is due to the bending in-plane NC-C-NO vibrations [12]. The assignments of the peaks in the IR spectrum are also summarized in Table 2.

https://scilett-fsg.uitm.edu.my/
Science Letters, **14**(2): 71-84 (2020)
ISSN: 1675-7785
eISSN: 2682-8626
DOI: 10.24191/sl.v14i2.9544

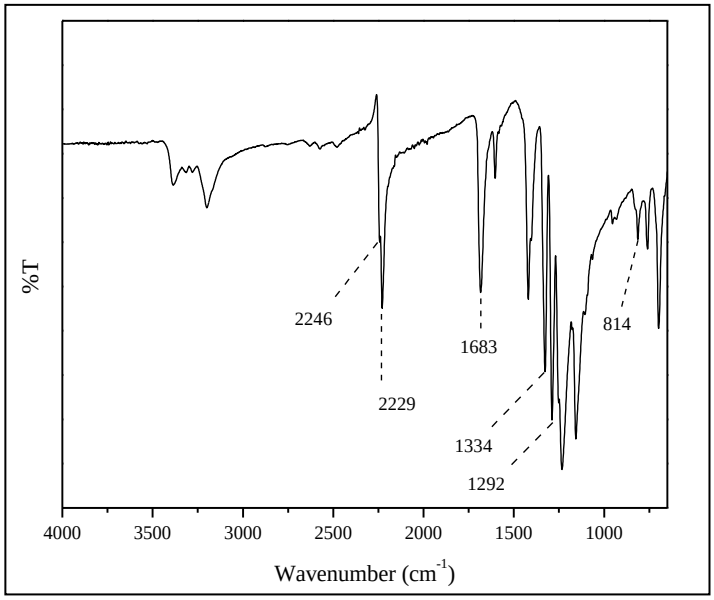

Figure 1: The FT-IR spectrum of $Ag[ONC(CN)_2]$ complex**.**

Table 2: The IR peaks and vibration mode of $Ag[ONC(CN)_2]$ complex [12].

FTIR Peak (cm^{-1})	Vibrational mode
2246 2229	Stretching vibration of ν(C ≡ N) of the cyano group.
1334	In-plane stretching vibrations ν(C-N) and ν(N-O) and bending vibration δ(C-N-O) of the nitroso group.
1292	in-plane stretching vibrations ν(C=N) and the bending vibration δ(C-N-O) of the nitroso group
814	Bending in-plane NC-C-NO vibrations.

The UV-Vis spectrum of $Ag[ONC(CN)_2]$ is shown in Figure 2. A bright yellow color solution was obtained when the metal complex dissolved in CH_3CN. The peak around 390-450 nm corresponds to the $n \rightarrow \pi^*$ transition in the nitroso chromophore [12-13]. The data obtained matched with the data reported by Glover et al. [12]. Thus, confirming the synthesis of $Ag[ONC(CN)_2]$ complex.

https://scilett-fsg.uitm.edu.my/
Science Letters, **14**(2): 71-84 (2020)

ISSN: 1675-7785
eISSN: 2682-8626
DOI: 10.24191/sl.v14i2.9544

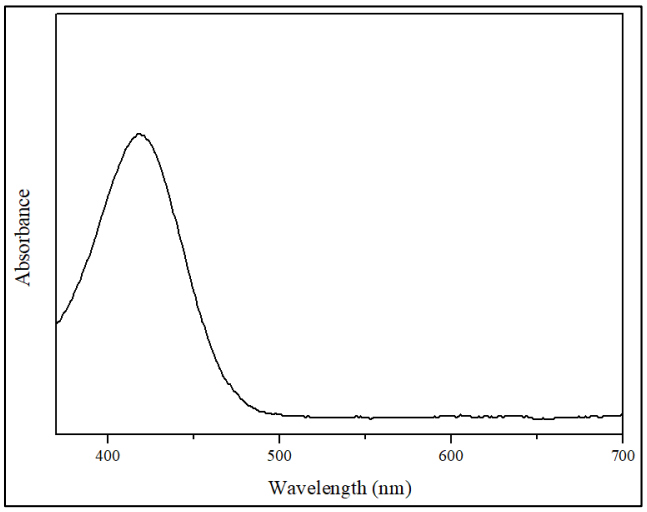

Figure 2: The UV-Vis spectrum of $Ag[ONC(CN)_2]$ complex.

Oxidation of styrene catalyzed by $Ag[ONC(CN)_2]$ complex

The color of the solution changed from yellow to colorless when H_2O_2 was added, indicating the change in the polarity of the reaction mixture. Since the polarities of the ground and excited state of a chromophore is different, a change in the solvent polarity will lead to different stabilization of the ground and excited states. This will result in a change in the energy gap between the electronic states thus changing the color of the solution [20]. This phenomenon is known as solvatochromism.

The progress of the Sty oxidation was monitored at different time intervals until 6 h at 353 K to evaluate the impact of reaction time on the catalytic activity of $Ag[ONC(CN)_2]$ complex. Figure 3 shows the changes in the conversion rate as well as the product selectivity. From the figure, increasing reaction time favored the conversion of Sty but reduced the product selectivity. In the first 3 h, the conversion of Sty reached 57% with 76% benzaldehyde (BZ) selectivity and 24% styrene oxide (StO) selectivity.

As the reaction time was prolonged, the Sty conversion remained constant (~62%). The BZ selectivity increased to 84% whereas, the selectivity of StO progressively decreased. The H_2O_2 molecules that were not coordinated with the Ag(I) active center will undergo self-decomposition forming hydroxyl radicals [21]. These hydroxyl radicals are capable of cleaving the C=C of the Sty side chain and the epoxy ring of styrene oxide to BZ [22, 23, 24]. Acetophenone (Ace) which can be formed from the direct oxidation of styrene started to form at 4 h [25]. The optimization of other parameters was carried out for 3 h due to the better product selectivity.

https://scilett-fsg.uitm.edu.my/
Science Letters, **14**(2): 71-84 (2020)
ISSN: 1675-7785
eISSN: 2682-8626
DOI: 10.24191/sl.v14i2.9544

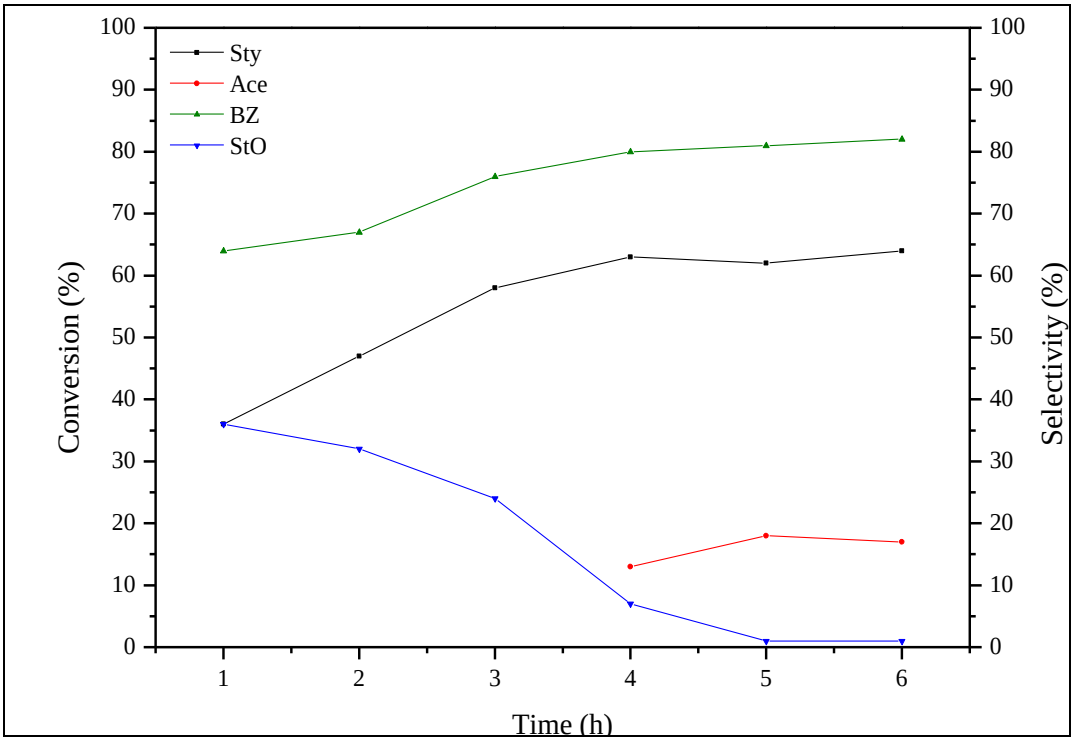

Figure 3: The conversion of Sty and the variation in product selectivity as a function of time. The mass of catalyst used was 50 mg. The reaction temperature was 353 K with 1:2 Sty: H_2O_2 molar ratio.

The influence of Sty:H_2O_2 molar ratio on the styrene conversion and product selectivity are presented in Table 3. The conversion of Sty remained 54-58% when H_2O_2 concentration was increased. Water is the only by-product produced from the use of H_2O_2 [26]. As the H_2O_2 concentration was increased, more water molecules will be generated. The water molecules can coordinate with the Ag(I) metal center and suppress the catalytic activity of the complex [17]. The selectivity of benzaldehyde increased ~20% when the molar ratio increased from 1:1 to 1:2 and remained constant (80%) with a subsequent increase. The selectivity of StO reduced rapidly to less than 10%. Ace started to form when the Sty:H_2O_2 molar ratio was increased to 1:3 and 1:4. Excess amounts of hydroxyl radicals generated from the self-decomposition of the uncoordinated H_2O_2 molecules may have oxidized the Sty to BZ and Ace. Based on the product selectivity, 1:1 styrene to H_2O_2 was considered the optimized molar ratio.

Table 4 shows the influence of the catalyst mass on the conversion of styrene and product selectivity. Increasing the mass of the catalyst while keeping 1:1 styrene to H_2O_2 molar ratio constant did not have any effect on the styrene conversion nor the product selectivity. In all cases, the selectivity of BZ and StO was found in an 80:20 ratio. Since a further increase in the catalyst mass did not result in any significant change in the Sty conversion or product selectivity, it is concluded that the added H_2O_2 was fully utilized and the excess catalyst was unused. Based on the collected data, the optimum catalyst mass was 25 mg.

https://scilett-fsg.uitm.edu.my/
Science Letters, **14**(2): 71-84 (2020)
ISSN: 1675-7785
eISSN: 2682-8626
DOI: 10.24191/sl.v14i2.9544

Table 3: Conversion of Sty and the variation in product selectivity at different Sty:H_2O_2 molar ratio. The mass of the catalyst used was 50 mg. The reaction was carried out at 353 K for 3 h.

Sty:H_2O_2 molar ratio	Conversion (%)	Selectivity (%)		
		Ace	BZ	StO
1:1	58	-	52	48
1:2	54	-	76	24
1:3	58	12	80	8
1:4	57	15	79	6

Table 4: Sty conversion and variation in BZ and StO selectivity as a function of mass. The reaction was carried out at 353 K for 3 h. Sty:H_2O_2 molar ratio used was 1:1.

Mass (mg)	Conversion (%)	Selectivity (%)	
		BZ	StO
25	57	81	19
50	58	76	24
75	58	79	21
100	57	80	20

The influence of temperature on the Sty conversion and product selectivity is shown in Table 5. The styrene conversion increased from 36% to 58% when the reaction temperature was increased from 303 to 353 K. The Ag(I) complex seems to be more selective at a lower temperature. Only BZ was obtained at 303 K, whereas at 333 K and 353 K, StO was obtained together with benzaldehyde. It has been reported that the decomposition of H_2O_2 at ~293-303 K was very slow but becomes rapid at higher temperature [27]. Due to the lower energy at 303 K, more H_2O_2 molecules were able to coordinate with Ag(I) metal center compared at higher temperatures. This observation indicate that at 303 K, the reaction did not proceed by hydroxyl radicals. However, due to high energy supply at 333 K and 353 K, the reaction could possibly be catalyzed predominantly by hydroxyl radicals.

In conclusion, to selectively oxidize Sty (10 mmol) to BZ, the reaction conditions required were: 25 mg catalyst, 10 mmol H_2O_2, 10 mL CH_3CN and the reaction was carried out at 303 K for 3 h. To investigate the contribution of hydroxyl radicals, a blank reaction (without catalyst) and a reaction in the presence of $C_6H_8O_6$ was carried out under the optimum conditions. The collected data are given in Table 6. The $C_6H_8O_6$ was added as a scavenger to capture hydroxyl radicals that were present in the reaction mixture; hence, suppressing the reaction if the reaction was catalyzed by hydroyxl radicals. Without the catalyst, only 12% of Sty was converted to BZ. This means only 12% of the Sty conversion is contributed by the hydroxyl radicals. In the presence of $C_6H_8O_6$ and the complex, 30% of styrene was converted, which is similar to the

https://scilett-fsg.uitm.edu.my/
Science Letters, **14**(2): 71-84 (2020)
ISSN: 1675-7785
eISSN: 2682-8626
DOI: 10.24191/sl.v14i2.9544

reaction without $C_6H_8O_6$. This means that at 303 K, in the presence of the complex, the reaction was not catalyzed by the hydroxyl radicals.

Table 5: Conversion and Sty and variation in BZ and StO selectivity at a different temperature. The mass of catalyst used was 25 mg. The reaction was carried out for 3 h with 1:1 Sty:H_2O_2 molar ratio.

Temperature (K)	Conversion (%)	Selectivity (%)	
		BZ	StO
303	36	100	-
333	46	88	12
353	58	81	28

Based on the results presented in Table 6, the reaction is proposed to take place *via* the formation of [Ag-H_2O_2] adduct. The Ag(I) is proposed to be the electrophile, whereas the oxygen atom of H_2O_2 was proposed to be the nucleophile. The proposed reaction mechanism is shown in Figure 4. The peroxyl group was activated through the formation of [Ag-H_2O_2] adduct. The allylic oxidation between the styrene side chain and the adduct will lead towards the formation of styrene oxide. In the presence of H_2O_2, the [Ag-H_2O_2] adduct can be regenerated. The regenerated adduct can react with the styrene oxide forming a transition state. The electron rearrangement and C–C bond cleavage will give BZ, water, and formaldehyde. Formaldehyde could not be detected during GC-FID and GC-MS analyses due to its low boiling point, so it might have evaporated before being detected [28, 2].

Table 6: Comparison of Sty conversion and product selectivity when the reaction was carried out in the presence of $C_6H_8O_6$ and blank.

Temperature (K)	Conversion (%)	Selectivity (%)	
		BZ	StO
303	36	100	-
$C_6H_8O_6$*	30	100	-
Blank*	12	100	-

*under the optimum conditions: 25 mg catalyst, 1:1 Sty:H_2O_2 molar ratio, 303 K, and 3 h of reaction time.

https://scilett-fsg.uitm.edu.my/
Science Letters, **14**(2): 71-84 (2020)
ISSN: 1675-7785
eISSN: 2682-8626
DOI: 10.24191/sl.v14i2.9544

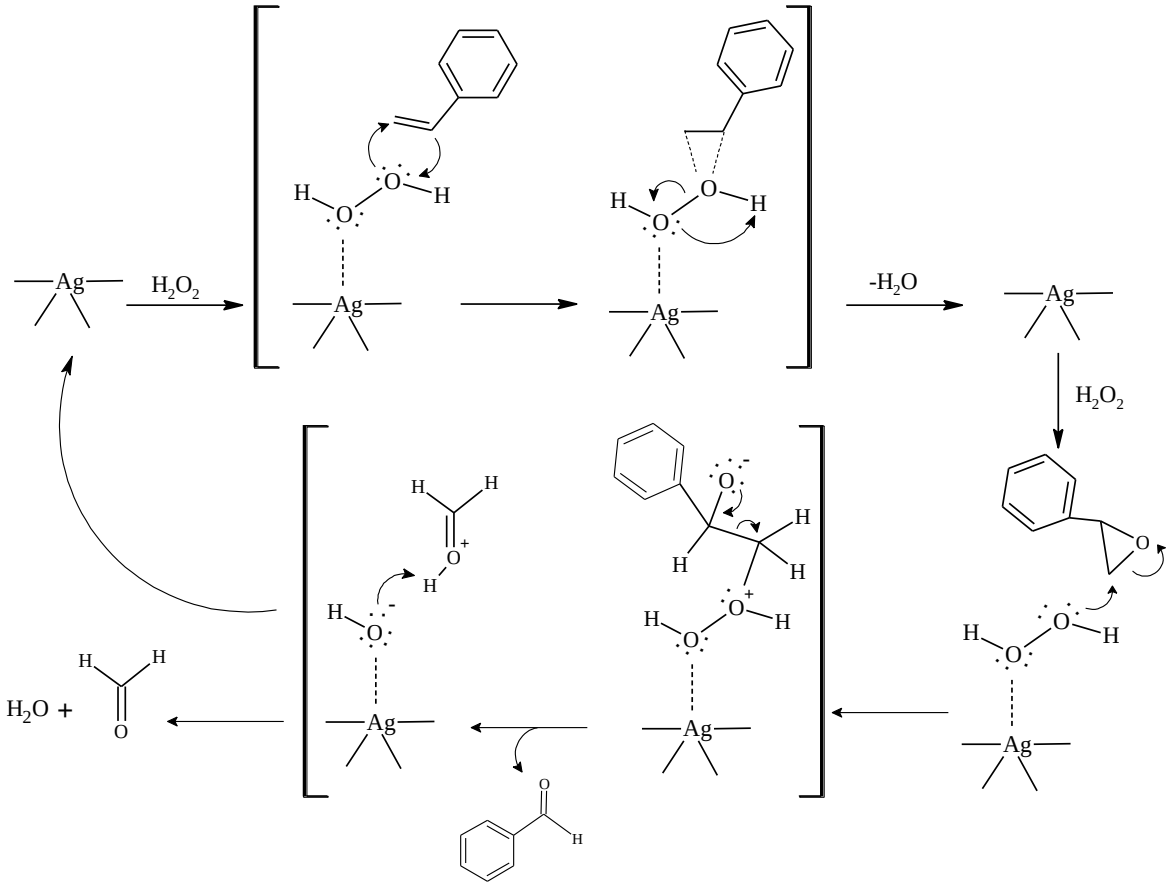

Figure 4: The possible reaction mechanism for the oxidation of styrene catalyzed by $Ag[ONC(CN)_2]$ complex.

The σ-profile of the complex and CH_3CN was constructed as in Figure 5. The σ-profile is defined as the probability distribution of surface charge density for a given molecule [17]. The σ-profile is related to the interaction of hydrogen bonds that determine the ability of the hydrogen to act as a donor or acceptor. The complex is considered polar when the screening charge density exceeds ± 0.008 e $Å^{-2}$. The CH_3CN had a peak beyond +0.008 e $Å^{-2}$, which represented the presence of a hydrogen bond and considered to be hydrogen bond acceptors. The complex has a broad and small shoulder extending from -0.25-0.15 e $Å^{-2}$. A similar trend was observed for CH_3CN. The collected data suggest that the main interaction favored by the complex was polar interaction or hydrogen bonding. The intermolecular hydrogen bond can be formed between the CH_3 fragment (red color) in CH_3CN and OCN fragment (blue color) of $Ag[ONC(CN)_2]$ (Figure 6).

https://scilett-fsg.uitm.edu.my/
Science Letters, **14**(2): 71-84 (2020)
ISSN: 1675-7785
eISSN: 2682-8626
DOI: 10.24191/sl.v14i2.9544

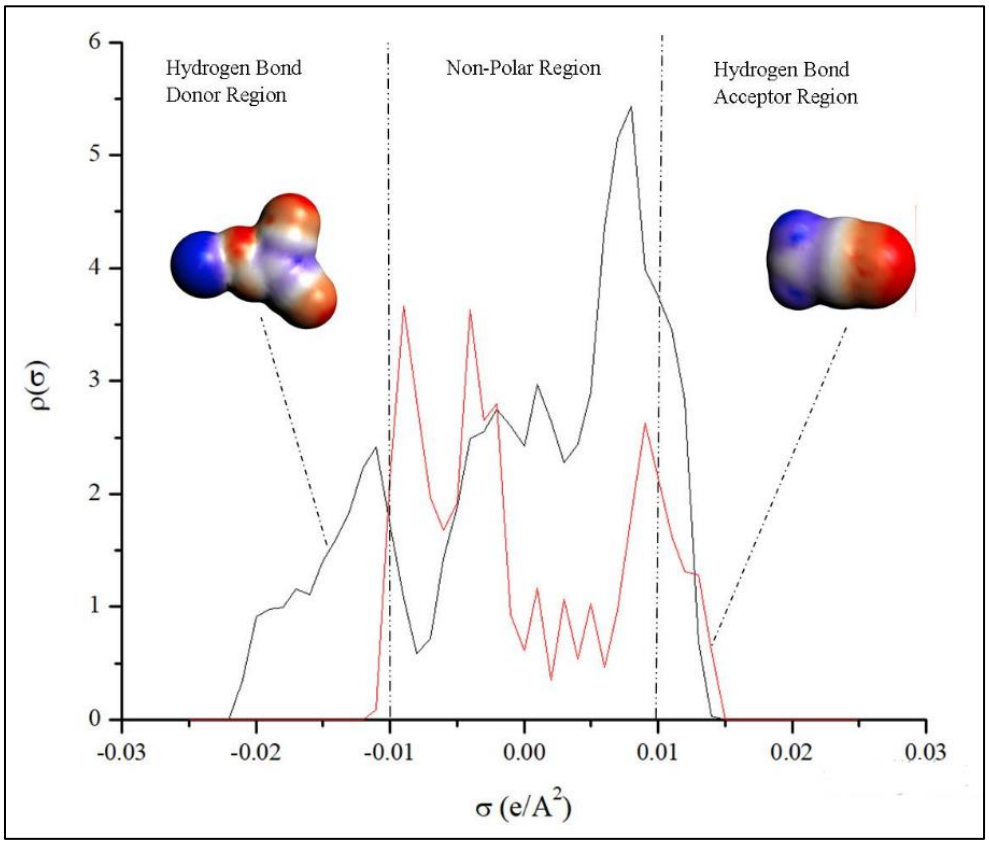

Figure 5: The σ-profile of a) Ag[ONC(CN)2] complex and b) CH3CN.

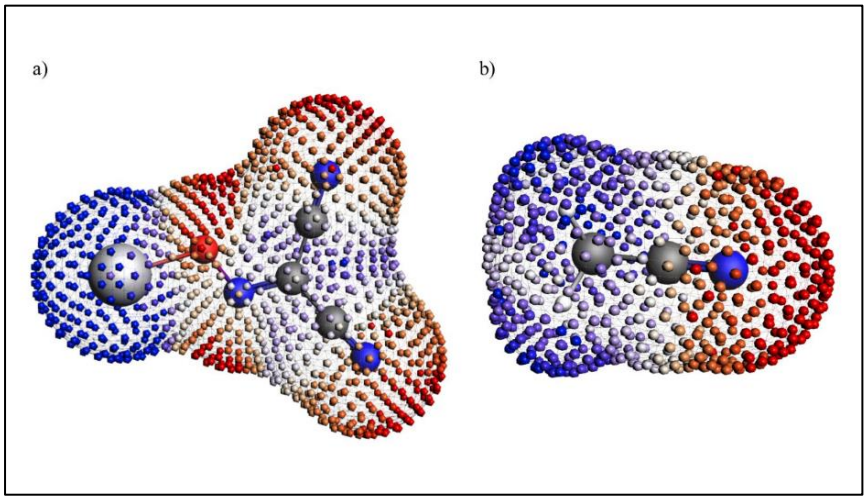

Figure 6: The COSMO-Surface charge density distribution of a) Ag[ONC$(CN)_2$] complex and b) CH_3CN.

https://scilett-fsg.uitm.edu.my/
Science Letters, **14**(2): 71-84 (2020)

ISSN: 1675-7785
eISSN: 2682-8626
DOI: 10.24191/sl.v14i2.9544

The MEP of the complex was calculated to visualize the electron distribution in the compound, as shown in Figure 7. The MEP visualization is widely used as a reactivity map displaying the electrophilic and nucleophilic attack regions and to identify the potential regions available for the interaction to occur [29]. The most nucleophilic regions (negative electrostatic potential) are shown in red, whereas the most electrophilic regions (positive electrostatic potential) appears in blue. The Ag(I) (0.577 a.u) appeared to be blue, indicating that it is the most electrophilic region of the $Ag[ONC(CN)_2]$ complex. The Ag(I) tends to accept the nucleophilic attack from the oxygen atom of H_2O_2. The interaction will form [Ag-H_2O_2] adduct, as shown in Figure 4. The MEP study confirms the proposed mechanism in Figure 4.

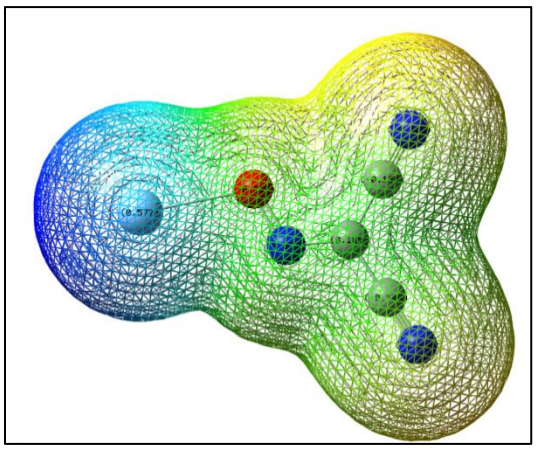

Figure 7: The molecular electrostatic potential (MEP) of $Ag[ONC(CN)_2]$ complex.

CONCLUSIONS

The $Ag[ONC(CN)_2]$ complex is capable of oxidizing styrene to benzaldehyde selectively. The optimum conditions required to oxidize styrene (10 mmol) were 25 mg catalyst, 10 mmol H_2O_2, 10 mL CH_3CN and the reaction carried out at 303 K for 3 h. The experimental and computational study indicate that the reaction takes place *via* the [Ag-H_2O_2] adduct. Under the optimum conditions, the conversion of Sty was 36%, with 100% selectivity towards BZ.

ACKNOWLEDGMENTS

The authors would like to thank the Malaysian Government and Universiti Sains Malaysia for sponsoring this work through Research University Grant (RUI) (1001/PKIMIA/8011083), International Islamic University Malaysia for Research Initiative Grant Scheme (IIUM) [RIGS 15-133-0133 and Universiti Kebangsaan Malaysian for Geran Universiti Penyelidikan Universiti Kebangsaan Malaysia (GUP-2019-045). The authors would like to thank Ministry of Education Malaysia (Higher Education) and Universiti Sains Malaysia for the Post-Doctoral Training Fellowship awarded to Anwar Iqbal.

https://scilett-fsg.uitm.edu.my/
Science Letters, **14**(2): 71-84 (2020)

ISSN: 1675-7785
eISSN: 2682-8626
DOI: 10.24191/sl.v14i2.9544

REFERENCES

[1] Tong, J., Li, W., Bo, L., Wang, H., Hu, Y., Zhang, Z., Mahboob, A., Selective oxidation of styrene catalyzed by cerium-doped cobalt ferrite nanocrystals with greatly enhanced catalytic performance. *Journal of Catalysis* **344**: 474–481 (2016).

[2] Oliveira, A.P.S., Gomes, I.S., Neto, A.S.B., Oliveira, A.C., Filho, J.M., Saraiva, G.D., Soares, J.M., Tehuacanero-Cuapa, S., Catalytic performance of MnFeSi composite in selective oxidation of styrene, ethylbenzene and benzyl alcohol. *Molecular Catalysis*, **436**: 29–42 (2017).

[3] Hu, Z., Zhao, Y., Liu, J., Wang, J., Zhang, B., Xiang, X., Ultrafine MnO_2 nanoparticles decorated on graphene oxide as a highly efficient and recyclable catalyst for aerobic oxidation of benzyl alcohol. *Journal of Colloid and Interface Science*, **483**: 26–33 (2016).

[4] Yadav, G.D., Haldavanekar, B.V., Mechanistic and kinetic investigation of liquid-liquid phase transfer catalyzed oxidation of benzyl chloride to benzaldehyde. *Journal of Physical Chemistry A*, **101**:36–48 (1997).

[5] Nasrollahzadeh, M., Bagherzadeh, M., Karimi, H., Preparation, characterization and catalytic activity of $CoFe_2O_4$ nanoparticles as a magnetically recoverable catalyst for selective oxidation of benzyl alcohol to benzaldehyde and reduction of organic dyes. *Journal of Colloid and Interface Science*, **465**: 271–278 (2016).

[6] Cheng, D.G., Chong, M., Chen, F., Zhan, X., XPS characterization of CeO_2 catalyst for hydrogenation of benzoic acid to benzaldehyde. *Catalysis Letter*, **120**: 82– 85 (2007).

[7] Lv, J., Shen, Y., Peng, L., Guo, X., Ding, W., Exclusively selective oxidation of toluene to benzaldehyde on ceria nanocubes by molecular oxygen. *ChemComm* **46**: 5909–5911 (2010).

[8] Cole-Hamilton, D.J., Homogeneous catalysis--new approaches to catalyst separation, recovery, and recycling. *Science*, **299**:1702-1706 (2003).

[9] Zhang, Y., Yang, T., Zheng, B., Liu, M., Xing, N., Synthesis, crystal structures of oxovanadium(V) complexes with hydrazone ligands and their catalytic performance for the styrene oxidation. *Polyhedron*, **121**: 123–129 (2017).

[10] Zhu, X., Shen, R., Zhang, L. Catalytic oxidation of styrene to benzaldehyde over a copper Schiff-base/SBA-15 catalyst. *Chinese Journal of Catalysis*, **35**: 1716–1726 (2014).

[11] Aragon-Muriel, A., Camprubi-Robles, M., Gonzalez-Rey, E., Salinas-Castillo, A., Rodriguez-Dieguez. A., Gomez-Ruiz, S., Polo-Ceron, D., Dual investigation of lanthanide complexes with cinnamate and phenylacetate ligands: Study of the cytotoxic properties and the catalytic oxidation of styrene. *Polyhedron*, **80**: 117–128 (2014).

[12] Glover, G., Gerasimchuk, N., Biagioni, R., Domasevitch, K.V., Monovalent K, Cs, Tl, and Ag Nitrosodicyanomethanides: Completely Different 3D Networks with Useful Properties of Luminescent Materials and Nonelectric Sensors for Gases. *Inorganic Chemistry*, **48**: 2371-2382 (2009).

[13] Bohle, D.S., Conklin, B.J., Hung. C.H. Coordination Chemistry of the pseudochalcogen nitrite analog nitrosodicyanomethanide. *Inorganic Chemistry*, **34**: 2569-2581(1995).

[14] Hvastijová, M., Koźíšek, J., Kohout, J., Mroziński, J., Jäger, L., Svododa, Polyhedron I Structural characterization of nitrosodicyanomethanide and dicyanamide complexes of copper(II), nickel(II) and cobalt(II) with imidazole and 1-methylimidazole. X-ray crystallographic evidence of unusual nitrosodicyanomethanide O-bonding in $Cu[ONC(CN)_2]_2$(1-methylimidazole)$_4$. *Polyhedron*, **16**: 463-471(1997).

[15] Arulsamy, N., Bohle, D.S., Doletski, B.G., Synthesis and thermal decomposition studies of new nitroso-and nitrodicyanomethanide salts. *Inorganic Chemistry*, **38**:2709-2715 (1999).

[16] Chow, Y.M., Britton, D., Silver dicyanonitrosomethanide, $AgC(CN)_2NO$. *Acta Crystallographica B*, 30:1117-1118

[17] Adam, F., Iqbal, A, The liquid phase oxidation of styrene with tungsten modified silica as a catalyst. *Chemical Engineering Journal*, **171**:1379– 1386 (2011).

[18] Normaya, E., Fazli, M., Ahmad, M.N., Ku Bulat, K.H., COSMO-RS and DFT studies on development and optimization of quercetin as a chemosensor for Fe^{3+} recognition in aqueous medium. *Journal of Molecular Structure*, **1184**: 538-545 (2019).

https://scilett-fsg.uitm.edu.my/
Science Letters, **14**(2): 71-84 (2020)

ISSN: 1675-7785
eISSN: 2682-8626
DOI: 10.24191/sl.v14i2.9544

[19] Normaya, E., Ahmad, M.N., Farina, Y., Ku Bulat, K.H. Synthesis, Characterization and Preliminary Study on Acetylpyrazine N(4)Butylthiosemicarbazone as a Potential CDK2 Inhibitor Combined with DFT Calculations. *Journal of the Brazillian Chemical Society* **29**: 2197-2206 (2018).

[20] Rauf, M.A., Hisaindee, S., Studies on solvatochromic behavior of dyes using spectral techniques. *Journal of Molecular Structure*, 1042: 45-46 (2013).

[21] Xue-jing, Y., Peng-fei, T., Xiao-man, Z., Xin, Y., Ting, W., Jing, X., Yi-fan, H. The generation of hydroxyl radicals by hydrogen peroxide decomposition on FeOCl/SBA-15 catalysts for phenol degradation. *AIChE Journal, 61:166-176 (2014).*

[22] Abdul L.A., Behnam, K., Subhash, B., Seng, B. O. Oxidation of styrene to benzaldehyde by anhydrous hydrogen peroxide on γ-alumina-supported V_2O_5 nanoparticle catalysts: optimization studies using response surface methodology. *International Journal of Applied Ceramic Technology, 9(3): 588-598 (2012).*

[23] Satoru, I., Yoshihiro, K., Takuya N., Dachao, H., Hideo, K., Daisuke, I., Kazuhiko S. Titania-Catalyzed H_2O_2 Thermal Oxidation of Styrenes to Aldehydes. *Molecules, 24(14): 1-9 (2019).*

[24] Ana, P. S. O., Igor, S. G., Alcineia, C. O., Josue, M. F., Gilberto, D. S., João, M. S., Francisco, F. S., Adriana, C. Styrene oxidation to valuable compounds over nanosized FeCo-based catalysts: effect of the third metal addition. *Catalysts*, **7**(11): 3-27 (2017).

[25] Yu, L., Ziming, Z., Li, W., Sha, L., He, W., Wei, W., Hongbo, Z., Jiantai, M. Distinctive ligand effects of functionalized magnetic microparticles immobilizing palladium acetate as heterogeneous coordination catalysts for selective oxidation of styrene to acetophenone. *Molecular Catalysis*, **433**: 291–300 (2017).

[26] Jiandi, L., Bangbang, H., Qiang, C., Junshuai, L., Qing, X., Guanghui, Y., Xianhui, Z., Size, Y., Hai, L., Qing, H.L. Direct synthesis of hydrogen peroxide from plasma-water interactions. *Scientific Reports*, **6**: 1-7 (2016).

[27] Ersin, Y., Deveci, H., Factors affecting decomposition of hydrogen peroxide, in Proceedings of the XII International Mineral Processing Symposium (IMPS), 6 to 8 Ocober 2010, Cappadocia- Nevsehir, Turkey, O. Y. Gulsoy, S. L. Ergun, N. M. Can, I. B. Celik, Eds. (Hacettepe University, Department of Mining Engineering, 2010), pp. 609–616.

[28] Dong, J.J., Saisaha, P., Meinds, T.G., Alsters, P.L., Ijpeij, E.G., van Summeren, R.P., Mao, B., Fañanás-Mastral. M., de Boer, J.W., Hage, R., Feringa, B.L., Browne, W.R., Oxidation of alkenes with H_2O_2 by an in-situ prepared Mn (II)/pyridine-2-carboxylic acid catalyst and the role of ketones in activating H_2O_2. *ACS Catalysis*, **2**(6): 1087-1096 (2012).

[29] Pawar, R.Y., Pardeshi, S.K., Selective oxidation of styrene to benzaldehyde using soft $BaFe_2O_4$ synthesized by citrate gel combustion method. *Arabian Journal of Chemistry*, **11**(2): 282-290 (2014).